

Zero-averaged refractive-index gaps extension by using photonic heterostructures containing negative-index materials

H.Y. Zhang · Y.P. Zhang · W.H. Liu · Y.Q. Wang · J.G. Yang

Received: 8 November 2008 / Published online: 28 February 2009
© Springer-Verlag 2009

Abstract We show theoretically that the frequency range of the zero-averaged refractive-index gap can be substantially extended in a photonic heterostructure containing negative-index materials. This photonic heterostructure consists of different one-dimensional (1D) photonic crystals. The constituent 1D photonic crystals have to be properly chosen in such a way that their zero-averaged refractive-index gap of the adjacent photonic crystals overlap each other.

PACS 42.70.Qs · 42.82.Et

1 Introduction

Conventional photonic band-gap (PBG) materials are a type of artificial composites with periodically modulated dielectric function, and the photonic gaps are a consequence of Bragg scattering in these materials [1, 2]. Recently, left-handed materials (LHMs) with simultaneously negative permittivity and negative permeability, yielding a negative refractive index, have been extensively studied in several distinct artificial physical settings inspired by Veselago's work many years ago [3]. Left-handed materials exhibit new properties which originated the zero-averaged index gap (ZAIG) from the one-dimensional photonic crystal (1DPC) containing positive- and negative-index material. This ZAIG is invariant upon the change of scaling, insensitive to the disorder, and also independent of the incident angle and polarization [4–6]. Such a zero- \bar{n} gap has many different properties

from the usual photonic band gaps (PBGs) induced by the Bragg scattering. The width of the ZAIG plays an important role in the application of 1DPC omnidirectional reflectors. However, the width of the ZAIG is very narrow making these structures inefficient in application as omnidirectional total reflectors.

It has been demonstrated that it is possible to enlarge the total reflection frequency range by combining two or more photonic crystals (PCs) (photonic heterostructures) for 1D and 2D PCs in the case of normal incidence [7, 8]. The idea has been successfully applied to acoustic band-gap materials [9]. In this letter, we show theoretically that by combining two 1DPCs containing negative-index materials (NIMs) and positive-index materials (PIMs) to form photonic heterostructures it is possible to enlarge the total reflection frequency range of ZAIG. The key idea is that the ZAIG of the neighboring PCs overlap each other.

2 Computational model and numerical method

The calculated schematic is shown in Fig. 1. $(AB)_m$ and $(A'B')_n$ are two different 1D photonic crystals containing NIMs and PIMs. $A(A')$ and $B(B')$ indicate NIMs and PIMs, respectively. $m(n)$ is the period number. In the following numerical investigation, a NIMs is assumed to be isotropic and dispersive with effective ε and μ given by

$$\varepsilon(\omega) = \varepsilon - \frac{\alpha}{\omega^2}, \quad (1)$$

$$\mu(\omega) = \mu - \frac{\beta}{\omega^2}. \quad (2)$$

In (1) and (2), ω is the frequency measured in GHz. In our calculation, we have chosen $\varepsilon = 1.21$, $\mu = 1.0$, $\alpha =$

H.Y. Zhang (✉) · Y.P. Zhang · W.H. Liu · Y.Q. Wang · J.G. Yang
College of Science, Shandong University of Science and
Technology, Qingdao, Shandong, 266510, China
e-mail: huiyunzhang1019@yahoo.com.cn

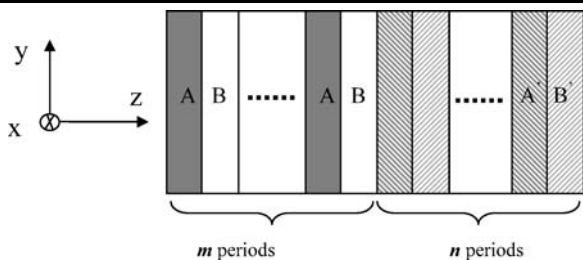


Fig. 1 Schematic of a heterostructure constituted by two different 1D photonic crystals $[(AB)_m \text{ and } (A'B')_n]$ with NIMs

$\beta = 100$. The thickness and refractive index of NIMs and PIMs slabs in the two photonic crystals are assumed to be $d_A, d_B, d_{A'}, d_{B'}$, and $n_A(\omega) = -\sqrt{\varepsilon(\omega)\mu(\omega)}, n_B$, respectively. Here, we use $d_A = 24$ mm, $d_B = 48$ mm, $d_{A'} = 24$ mm, $d_{B'} = 16$ mm, $n_B = 2.0$, and $m = n = 20$.

Let a wave incident from a vacuum at an angle θ onto a heterostructure constituted by two different 1D photonic crystals $[(AB)_m \text{ and } (A'B')_n]$ with NIMs and PIMs, as show in Fig. 1. For the transverse electric (TE) wave, the electric field \mathbf{E} is assumed in the x direction (the dielectric layers are in the x - y plane), and the z direction is normal to the interface of each layer. In general, the electric and magnetic fields at any two positions z and $z + \Delta z$ in the same layer can be related via a transfer matrix [5, 6]:

$$M(\Delta z, \omega) = \begin{pmatrix} \cos[k_z \Delta z] & i \frac{\mu}{\sqrt{\varepsilon\mu - \sin^2 \theta}} \sin(k_z \Delta z) \\ i \frac{\sqrt{\varepsilon\mu - \sin^2 \theta}}{\mu} \sin(k_z \Delta z) & \cos[k_z \Delta z] \end{pmatrix}, \quad (3)$$

where $k_z = \omega/c\sqrt{\varepsilon_j}\sqrt{\mu_j}\sqrt{1 - (\sin^2 \theta/\varepsilon_j\mu_j)}$ is the z component of the wave vector k^j in the j th layer, and c is the speed of light in vacuum. Then the transmission coefficient $t(\omega)$ can be obtained from the transfer matrix method [6],

$$t(\omega) = \frac{2 \cos \theta}{(m_{11} + m_{22}) \cos \theta + i(m_{12} \cos^2 \theta - m_{21})}. \quad (4)$$

Here $m_{ij}(\omega)$ ($i, j = 1, 2$) is the matrix element of $X_N(\omega) = \prod_{j=1}^N M_j(d_j, \omega)$ which represents the total transfer matrix connecting the fields at the incident end and the exit end. The treatment for a TM wave is similar to that for a TE wave.

For an infinite periodic structure, based on theorem and boundary condition, the dispersion relation at any incident as

$$\cos(q_z d) = \cos(k_z^A d_A) \cos(k_z^B d_B) - \frac{1}{2} \left(\frac{p_B}{p_A} + \frac{p_A}{p_B} \right) \sin(k_z^A d_A) \sin(k_z^B d_B), \quad (5)$$

where q_z is the z component of the Bloch wave vector.

3 Results and discussion

Photonic band structures in terms of frequency and incident angle for the two PCs, obtained from (5), are shown in Fig. 2; electromagnetic wave incident from air. It can be seen from Fig. 2a that the upper band edge is sensitive to the increase of the incident angle for both polarizations, and the frequency shift of the lower band edge for TE mode is upward to high frequency as the incident angle increases, and the lower band edge is insensitive to the increase of the incident angle for TM mode. There is an omnidirectional PBG for the TE polarization in the displayed frequency range, from 3.92 to 5.35 GHz. For the TM polarization, the omnidirectional PBG spans from 3.65 to 5.35 GHz. We thus can obtain the overall frequency range of the omnidirectional PBG for any polarization from 3.92 to 5.35 GHz, and the frequency bandwidth is $\Delta\omega = 1.43$ GHz.

In Fig. 2b, we can see that the band gap of TM polarization is very sensitive to the increase of the incident angle, which is different from the case in PC1. There is an omnidirectional PBG for the TE polarization in the displayed frequency range, from 5.32 to 7.63 GHz. For the TM polarization, the omnidirectional PBG spans from 5.2 to 6.52 GHz. We thus can obtain the overall frequency range of the omnidirectional PBG for any polarization from 5.32 to 6.52 GHz, and the frequency bandwidth is $\Delta\omega = 1.2$ GHz.

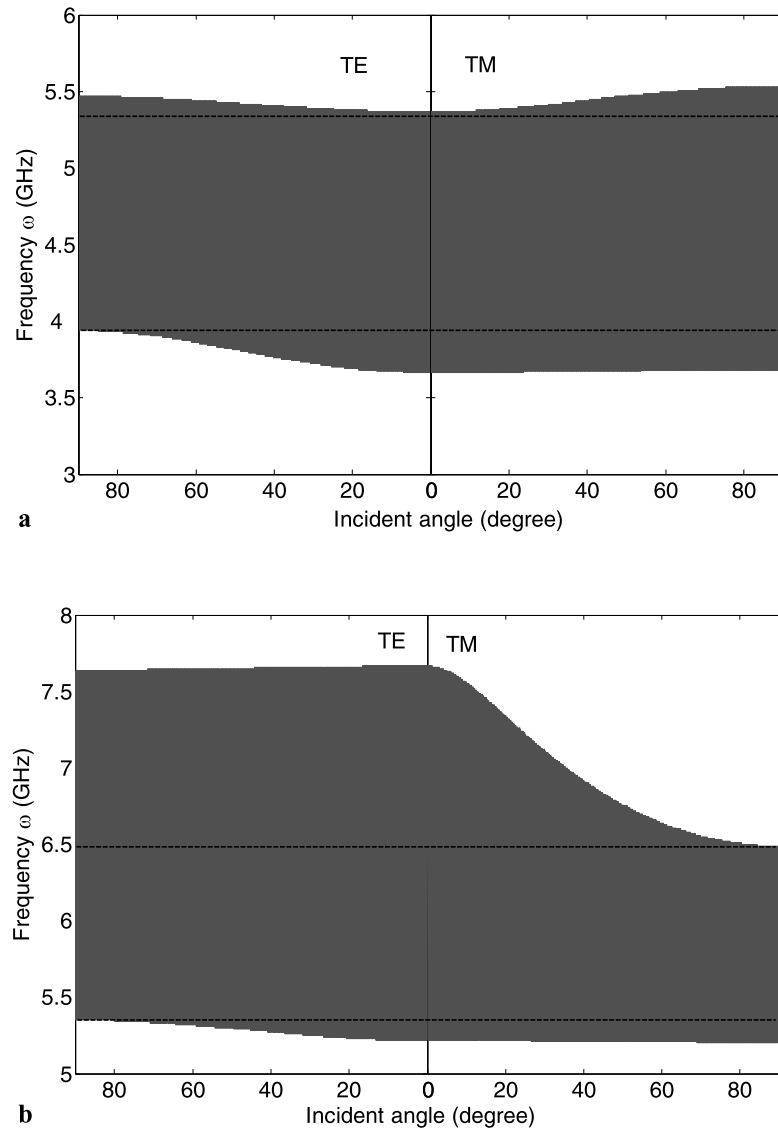
It can be seen from Fig. 2 that the directional PBGs for PC1 and PC2 overlap each other at any incident angle. This kind of lineup of PBGs, similar to the type-II lineup of the band gaps in semiconductor heterostructures, is crucial for the enlargement of the omnidirectional total reflection by using two or more PCs to form photonic heterostructures. At any incident angle, incident EM waves with frequency located in the directional PBGs of the constituent PCs can not propagate in the photonic heterostructure. As a result, the frequency range of total reflection in some sense is enlarged for all incident angles.

To show the photonic heterostructure can enlarge the omnidirectional total reflection frequency range, transmission spectra of the constituent PCs and their resulting photonic heterostructure for both TE and TM polarizations at different incident angles are given in Fig. 3. The spectra are calculated by using a transfer matrix method.

For normal incidence, the TE and TM polarizations are degenerate. For PC1, the total reflection frequency range is about from 3.62 to 5.38 GHz. For PC2, the range is about from 5.21 to 7.63 GHz. After forming the photonic heterostructure by stacking PC1 and PC2 together (denoted by PC1/PC2), the enlarged total reflection frequency range is finally from 3.62 to 7.63 GHz.

At the incident angle of 45° , for PC1, the total reflection frequency range is from 3.81 to 6.86 GHz. For PC2,

Fig. 2 Photonic band structures of (a) PC1 and (b) PC2 in terms of angular frequency and incident angle. The *gray areas* represent forbidden bands. The frequency range between two *dashed lines* in the gray area is the total omnidirectional band gap



the range is from 5.36 to 6.86 GHz. For the photonic heterostructure PC1/PC2, the enlarged total reflection frequency range spans from 3.81 to 6.86 GHz.

At the incident angle of 89° , for PC1, the total reflection frequency range is from 3.92 to 5.48 GHz. For PC2, the range is from 5.23 to 6.52 GHz. For the photonic heterostructure PC1/PC2, the enlarged total reflection frequency range spans from 3.92 to 6.52 GHz.

From the aforementioned discussions, the total reflection frequency range is substantially enlarged for all incident angles and for both TM and TE polarizations. Consequently, the omnidirectional total reflection frequency range for any polarization is enlarged. It is obvious that one can use more 1D PCs to form multiple photonic heterostructures to get a very wide omnidirectional total reflection frequency range as desired provided that the directional PBGs of the adjacent

1D PCs at any incident angle overlap each other in tandem. The wider-bandwidth ZAIG has potential applications in microcavities, antenna substrates, and coaxial waveguides, etc.

4 Conclusions

In summary, we have demonstrated that the zero-averaged refractive-index gap can be enlarged as desired by using different PCs to form multiple heterostructures with their non-transmission ranges properly arranged. The idea to use photonic multiple heterostructures may provide a simple and effective way to solve the problem of enlarging the frequency range of zero-averaged refractive-index gap, which may have potential applications in improving planar microcavities, optical fibers, and Fabry–Perot resonators, etc.

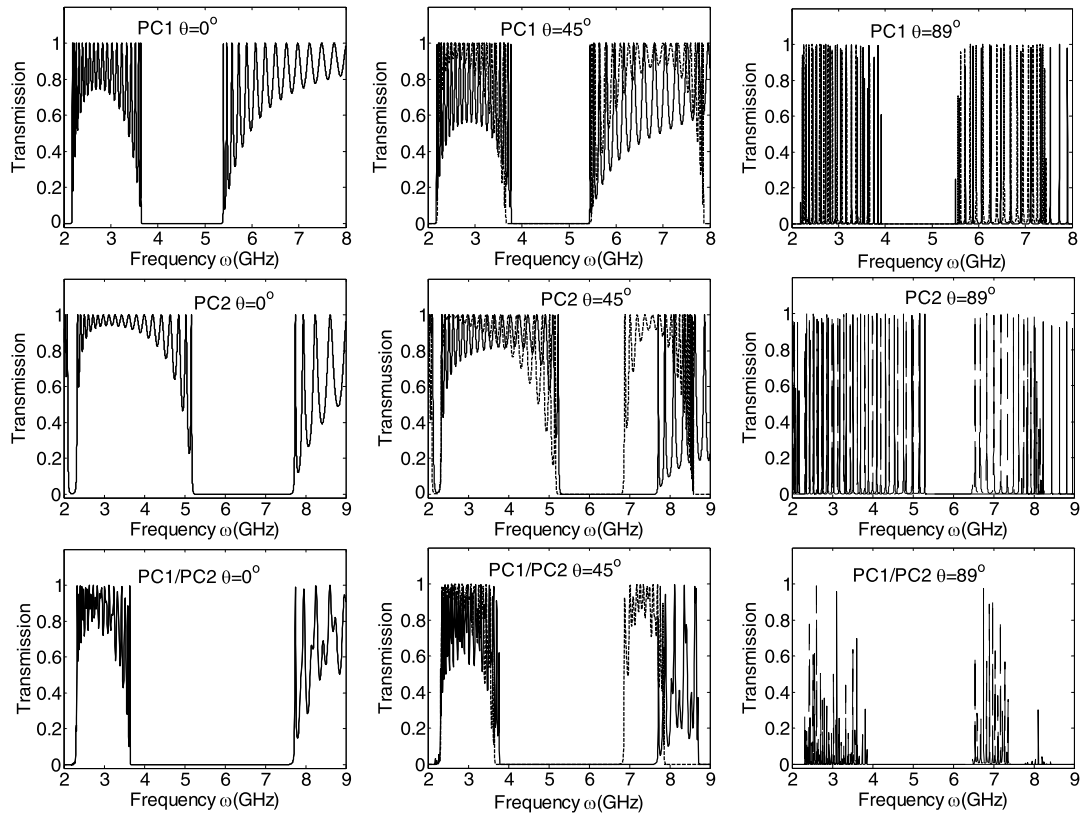


Fig. 3 Calculated transmission of PC1, PC2, and the heterostructure PC1/PC2 at different incident angles. The *solid* and *dotted lines* stand for TE and TM polarizations, respectively. Note that at normal incidence TE and TM polarizations are degenerate

Acknowledgement This work was supported by the National Natural Science Foundation of China (Grant No. 60671036) and the Research Project of “SUST Spring Bud” (Grant No. 2008AZZ094).

References

1. E. Yablonovitch, Phys. Rev. Lett. **58**, 2059 (1987)
2. S. John, Phys. Rev. Lett. **58**, 2486 (1987)
3. V.G. Veselago, Sov. Phys. Usp. **10**, 509 (1968)
4. J. Li, L. Zhou, C.T. Chan, P. Sheng, Phys. Rev. Lett. **90**, 083901 (2003)
5. L.G. Wang, H. Chen, S.Y. Zhu, Phys. Rev. B **61**, 10762 (2000)
6. H.T. Jiang, H. Chen, H.Q. Li, Y.W. Zhang, S.Y. Zhu, Appl. Phys. Lett. **83**, 5386 (2003)
7. J. Zi, J. Wan, C. Zhang, Appl. Phys. Lett. **73**, 2084 (1998)
8. C. Zhang, F. Qiao, J. Wan, J. Zi, J. Appl. Phys. **87**, 3174 (2000)
9. D. Bria, B. Djafari-Rouhani, A. Bousfia, E.H. El Boudouti, A. Nougouai, Europhys. Lett. **55**, 841 (2001)